Ab-initio Transport Calculations for Single-atom Copper Junctions in the Presence of Hydrogen Chloride

Paul Schnäbele,[†,‡] Richard Korytár,[*,¶] Alexei Bagrets,[†] Tanglaw Roman,[§] Thomas Schimmel,[‖,†,⊥] Axel Groß,[§] and Ferdinand Evers[†,‡,⊥]

Institute of Nanotechnology, Karlsruhe Institute of Technology, Campus North, D-76344 Karlsruhe, Germany, Institut für Theorie der Kondensierten Materie, Karlsruhe Institute of Technology, Campus South, D-76128 Karlsruhe, Germany, Institute of Nanotechnology, Karlsruhe Institute of Technology, Campus North, D-76344 Karlsruhe, Germany, Institute of Theoretical Chemistry, Ulm University, 89069 Ulm, Germany, Institute of Applied Physics, Karlsruhe Institute of Technology, Campus South, D-76131 Karlsruhe, Germany, and Center of Functional Nanostructures, Karlsruhe Institute of Technology, Campus South, D-76131 Karlsruhe, Germany

E-mail: richard.korytar@kit.edu

[*]To whom correspondence should be addressed

[†]Institute of Nanotechnology, Karlsruhe Institute of Technology, Campus North, D-76344 Karlsruhe, Germany

[‡]Institut für Theorie der Kondensierten Materie, Karlsruhe Institute of Technology, Campus South, D-76128 Karlsruhe, Germany

[¶]Institute of Nanotechnology, Karlsruhe Institute of Technology, Campus North, D-76344 Karlsruhe, Germany

[§]Institute of Theoretical Chemistry, Ulm University, 89069 Ulm, Germany

[‖]Institute of Applied Physics, Karlsruhe Institute of Technology, Campus South, D-76131 Karlsruhe, Germany

[⊥]Center of Functional Nanostructures, Karlsruhe Institute of Technology, Campus South, D-76131 Karlsruhe, Germany

Abstract

We study the transport properties of single-atom thick Cu-wires submerged in an electrochemical solvent containing HCl. As a first step, we investigate the stability of hydrogen co-adsorbing with chlorine on the Cu(111) surface in an implicit electrochemical environment. We find that adding hydrogen to a Cl-covered Cu surface is energetically unfavorable. The result serves as an estimate for the number of Cl-atoms that adsorbs near the single-atom wire. We use it in order to construct model junctions (Cu-wire plus adsorbates) the transport properties of which we investigate with density functional theory (DFT). We find that the Cl and H adsorbates tend to deplete the density of states of the Cu-wire near the Fermi energy. As a consequence, the transmission is reduced. Interestingly, we observe that in the case of H-adsorption the amount of depletion is quite sensitive to the wire geometry (relaxed vs unrelaxed), while this is not the case with Cl.

Keywords

Helmholtz double-layer, electrochemical gating, nano-scale junction, ab-initio transport calculations

Introduction

The controlled manipulation of charge transport through atomic and molecular wires continues to be a significant experimental challenge. Essentially, the difficulties and the fascination associated with this research field emerge from the same fundamental fact: small changes on atomistic scales can significantly alter the junction's functionality. One of the control strategies that is successful even on the atomistic scale operates in electrochemical environments. It embarks on the possibility to manipulate the Helmholtz-double-layer (HDL) via the third (electrochemical) electrode potential. (The HDL forms at the interface between

the source/drain-electrodes, i.e. the wire and the solvent. It consists of physisorbed solvent particles together with the genuine wire surface.)

The technique has been employed previously in order to realize single atom switches (single-atom transistors[1]), but also molecular switches have been operated in this way.[2–4]

Due to this success it is at least conceivable that electrochemical control might be a successful strategy for operating nanosystems also in a broader scope, such as transport control in nanoporous media (through opening and closing of current bottlenecks).[5] Moreover, transport of charge close to nanostructured electrochemical interfaces is also an issue for battery materials.[6]

Despite the fundamental role of charge transport near electrochemical interfaces, the research area is still in its infancy. In part this is due to the fact that the inner structure of the HDL is difficult to investigate and by and large not very well understood. It is considerably challenging to investigate experimentally, but first steps in this direction have been made.[7] At present, the main understanding relies on macroscopic ideas, such as incorporated in the Gouy-Chapman theory.[8,9] Due to recent developments in computational high-performance ab-initio codes, some of the most pressing questions have become amenable to computer simulations. But clearly, in the absence of specific experimental data to validate the computational assumptions, the building of effective microscopic models still is a very challenging task.

In this work, we investigate the charge transport through single-atom copper wires in an electrochemical environment that contains HCl. Our goal is to qualitatively understand the physical mechanism that is most important for the electro-chemical control of the wire's conductance. To this end we employ the density functional theory (DFT) in order to estimate the typical coverage of the junction with Cl and H atoms in and near the thermodynamic equilibrium. We find that on flat surfaces (Cu(111)) under ambient conditions there is a wide window of electrode potentials in which the Cl-coverage is 1/3, i.e. there is a single Cl-atom per three surface Cu-atoms. Our calculations suggest that there is no hydrogen in

the immediate vicinity of the Cu-surface under the aforementioned conditions.

Based on this information about the relevant structural elements of the Helmholtz layer, reasonable configurations of Cl-adatoms can be chosen that serve as input for Kohn-Sham (KS) based transport studies. The transport calculations indicate that there is a strong impact of the Cl-atoms reducing the conductance of the Cu-wire. The effect can be interpreted as a depletion of the wire's local density of states (LDoS) near the Fermi energy due to the binding of the Cl adsorbates. In the absence of Cl, we find a similar transmission reduction induced by adsorbing H atoms. Interestingly, we observe that the strength of the suppression is very sensitive to the deformation of the wire's geometry after the adatoms have been adsorbed.

Methods and results

Surface morphology of Cu(111) in Cl-containing environment

A crucial quantity for the simulations is the number of chlorine atoms adsorbed on the copper junction under electrochemical conditions. In order to estimate this number, density functional theory (DFT) calculations were performed for flat Cu(111) electrodes. The (111) surface was modeled by a slab with five atomic layers in a periodic supercell implementation of DFT. The slab surfaces were separated by 25 Å wide vacuum regions. For the adsorption energetics, the two bottom atomic layers were fixed at bulk atomic separation, allowing the rest of the metal atoms to relax together with the adatoms.

All calculations were carried out using the DFT code VASP.[10] Electron-electron exchange and correlation interactions within the generalized gradient approximation were included in the calculations using the PBE functional.[11] The interaction between electrons and ions was described by the projector-augmented wave (PAW) method[12] as implemented by Kresse and Joubert.[13] Electronic wave functions were expanded in terms of a discrete plane-wave basis set with kinetic energies of up to 400 eV. Calculations were performed using a $2\sqrt{3} \times 2\sqrt{3}$

surface unit cell. For the integration over the first Brillouin zone, we used a mesh of $4 \times 4 \times 1$ special k-points[14] with a Methfessel-Paxton smearing[15] of 0.1 eV. Geometry optimizations were terminated once the forces on relaxed chlorine and copper atoms became less than 0.01 eV/Å.

Since we are modeling the adsorption in an electrochemical environment, the reference for the adsorption energy is the corresponding hydrated species in the electrolyte. This requires in principle the determination of solvation energies which can be quite cumbersome. Some estimate to derive the adsorption energies of solvated Cl^- and H^+ ions can be made via a thermodynamics cycle.[16,17]

However, there is a more elegant way to calculate the energies of solvated species using the concept of what is now coined the computational hydrogen electrode.[18,19] Within this approach, the electrolyte is viewed as a thermodynamical reservoir for the adsorbates and the fact is used that at the redox potential and standard conditions the solvated species is in equilibrium with the corresponding species in gas phase.

This approach has recently be used to determine the equilibrium coverage of halides on Cu(111) and Pt(111) as a function of the electrode potential.[20] We illustrate this method for the chloride adsorption. At the redox potential of the chlorine, the chloride anion is in equilbrium with the chlorine molecule Cl_2 in gas phase. Furthermore, it is known how the electrochemical potential of the chloride changes with the electrode potential and the

Table 1: Adsorption energies $E_{\mathbf{ads}}$ in eV for H, Cl adsorption on Cu(111) at different coverages (in ML) and positions

	top	fcc	hcp
$\Theta_{\mathrm{H}} = 1/12$	+0.35	−0.23	−0.23
$\Theta_{\mathrm{H}} = 1/3$	+0.40	−0.22	−0.23
$\Theta_{\mathrm{H}} = 1$	+0.71	−0.17	−0.17
$\Theta_{\mathrm{Cl}} = 1/12$	−1.51	−1.89	−1.88
$\Theta_{\mathrm{Cl}} = 1/3$	−1.40	−1.84	−1.84

concentration, namely according to

$$\tilde{\mu}(\mathrm{Cl^-(aq)}) - \mu(e^-) = \frac{1}{2}\mu(\mathrm{Cl_2(g)}) + e(U_{\mathrm{SHE}} - U^0) + k_{\mathrm{B}}T \ln a_{\mathrm{Cl^-}} \ , \tag{1}$$

where U^0 is the reduction potential of the chloride and $a_{\mathrm{Cl^-}}$ its activity coefficient. The free energy of adsorption as a function of the electrode potential at standard conditions can then be calculated acoording to

$$\Delta\gamma(U_{\mathrm{SHE}}) = \frac{N_{\mathrm{ads}}}{A_s}\left(E_{\mathrm{ads}} - e(U_{\mathrm{SHE}} - U^0) - k_{\mathrm{B}}T \ln a_{\mathrm{Cl^-}}\right) \ , \tag{2}$$

where the adsorption energy E_{ads} in Eq. 2 is taken with respect to the chlorine molecule in the gas phase. Thus this approach avoids to derive solvation energies as a reference for adsorption energies .[18] The same formalism applies to the adsorption of the H^+ where also the energy of the free H_2 molecule can be used as a reference. Thus we will in the following discuss the adsorption energy E_{ads} with respect to the free molecular species.

First, separate calculations for H-covered and Cl-covered copper surfaces have been performed at different coverages. The adsorption energies that are listed in Table 1 were calculated with regard to the respective free molecules,

$$E_{\mathrm{ads}} = \frac{E_{\mathrm{X/Cu}} - (E_{\mathrm{Cu}} + \frac{N}{2}E_{\mathrm{X_2}})}{N}, \tag{3}$$

where X =H,Cl, and N is the number of adatoms in the supercell. The calculated energies agree well with previous studies.[21–23] For both adsorbates, the most stable adsorption sites are the threefold hollow sites with the fcc and hcp threefold hollow sites being energetically almost degenerate. Calculations for 1/9 coverage on seven-layer symmetric slabs[24] confirm that the hollow sites are energetically equivalent for Cl adsorption on Cu(111). Adsorption becomes weaker with increasing coverage, suggesting that the interaction of adatoms among themselves is repulsive on the metal surface.

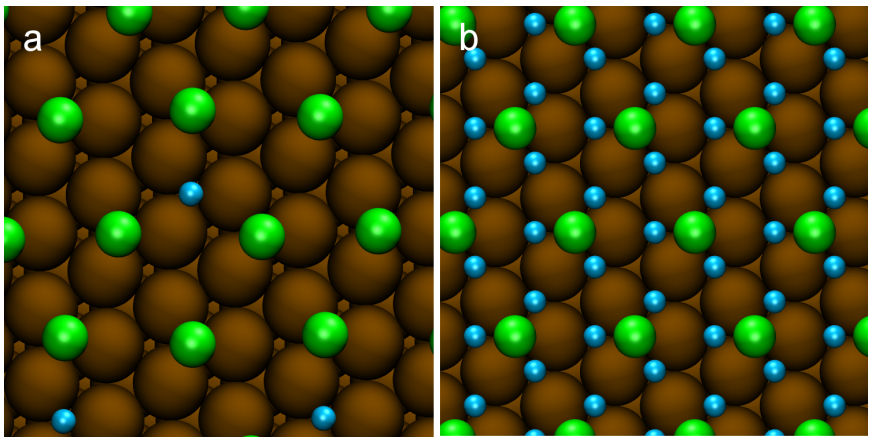

Figure 1: Co-adsorbed H with 1/3 ML Cl on Cu(111): (a) 1/12 ML H, (b) 1 ML H.

From Table 1, it is clear that the adsorption of chlorine is much stronger than hydrogen ($\Delta E_{\mathrm{ads}} \sim 1.7$eV). Hence we assume that the presence of hydrogen hardly affects the adsorption of chlorine. Therefore we focus on the equilibrium coverage of chlorine on Cu(111), wherein the electrochemical environment is considered as a reservoir from which the adsorbates come. Using the concept of the computational hydrogen electrode,[18,19] it was already shown that over a wide range of electrode potentials a ratio of one adsorbed chlorine atom per three copper atoms is thermodynamically stable,[20] in agreement with the experiment.[25]

We considered two co-adsorption systems of hydrogen and chlorine on the flat copper surface shown in Fig. 1: co-adsorbed H with 1/3 ML Cl on Cu(111), for hydrogen surface coverages of 1/12 ML and 1 ML H (representing low and high amounts of additional hydrogen). These models are consistent with cyclic voltammetry measurements complemented with in situ STM of Cu(111) electrodes in dilute HCl solutions.[25,26] Guided by Table 1, we have chosen adsorption only on threefold hollow sites for the co-adsorption configurations considered.

Assuming chlorine is already present at the Cu surface, the energy associated with adding hydrogen to the surface is

$$E_{\mathrm{H}} = \frac{E_{(\mathrm{H+Cl})/\mathrm{Cu}} - (E_{\mathrm{Cl/Cu}} + \frac{N_{\mathrm{H}}}{2} E_{\mathrm{H_2}})}{N_{\mathrm{H}}}. \quad (4)$$

DFT calculations yield $E_{\mathrm{H}} = 0.15\,\mathrm{eV}$ and $0.59\,\mathrm{eV}$ for the addition of hydrogen at coverages of 1/12 and 1 ML, respectively.These adsorption energies are significantly more positive than the corresponding hydrogen adsorption on clean Cu(111) of $E_{\mathrm{H}} = -0.23\,\mathrm{eV}$ and $-0.17\,\mathrm{eV}$ at coverages of 1/12 and 1 ML, respectively (see Tab. 1). This indicates that there is a repulsive interaction between adsorbed hydrogen and chlorine[27] and that adsorbed hydrogen atoms are unstable with respect to the desorption if the Cu surface is already covered with chlorine.The positive adsorption energies indicate that there is a repulsive interaction between adsorbed hydrogen and chlorine[27] – adsorbed hydrogen atoms are unstable with respect to the desorption if the Cu surface is already covered with chlorine. This is consistent with the observation that in the hydrogen evolution reaction on Cu the Volmer step $\mathrm{H} + e \rightarrow \mathrm{H_{ad}}$ is the rate-limiting step.[28]

Knowing that (1) chlorine adsorbs much more strongly on the surface compared to H, (2) its equilibrium coverage is 1/3 ML, and (3) that adding hydrogen to this Cl-covered Cu surface is energetically unfavorable, we conclude that single-atom Cu wires in an electrochemical solvent containing HCl will have only adsorbed chlorine. Thus, this section's results provide an estimate for the number of Cl-atoms that adsorb near the single-atom wire.

Transport of Cu-wires in H- and Cl-containing environments

We now study the effect that H and Cl adatoms have on the transmission properties of a single-atom copper wire. Although we just have shown that under electrochemical conditions hydrogen adsorption on copper is rather unlikely, we consider the influence of adsorbed hydrogen on the transport properties of the junction as hydrogen is a common adsorbate under electrochemical conditions on other electrode metals such as platinum.[29] As a very rough estimate of the number of adatoms that adsorb near the junction, we will assume that also the Cu wire exhibits a coverage close to 1/3, i.e. about every third Cu atom binds to a Cl atom. Like in the previous section, we treat exchange and correlation in the

generalized gradient approximation (PBE functional[11]). For cluster-type transport studies, it is advantageous to switch from a plane-wave to a strictly localized basis on solving the Kohn-Sham equations. For this reason, we made use of the FHI-AIMS package.[30] We employed an optimized atom-centered basis set from the reference[30] of the size equivalent to standard double-ζ sets of quantum chemistry [the "light" settings]. Structure relaxations have been performed until all force components per atom fell below the threshold 0.01 eVÅ^{-1}.

Model structures and electron transport method

Structure optimization. To define representative structures for the transport calculations, we first choose a vacuum geometry for "clean" wire composed of few atoms and suitable model electrodes (pyramids). A catalogue of the possible choices for the latter has been proposed and tested in conjunction with the AITRANSS module for DFT-based transport calculations.[31–33]

When attaching the adatoms, the structure optimization proceeds in two steps. First, we start with an initial (guess) structure and perform a "constrained relaxation": all Cu atoms are constrained to their vacuum positions; only the adsorbate atoms are allowed to move. Second, the constraint on the central part of the Cu junction – both apices, the atom in the middle and the three-atoms-top layers of the pyramids – is released, while remaining electrode atoms were fixed. In Fig. 2 we show two examples of initial and final (unconstrained) geometries. Clearly, the final structure for an unconstrained optimization may depend on the initial position of the Cl atoms. Fig. 2(d) shows a metastable state. Its energy is about 1eV higher than the one of the structure shown in Fig. 2 (b).

Electron transport calculations. Transport calculations have been performed with the module AITRANSS.[31–33] It relies on the Landauer-theory with Kohn-Sham scattering states obtained from the underlying ground-state DFT calculation. For a basic discussion of KS-based scattering theory see, e.g.,[34] and references therein. We note that the cluster-type

transport calculations often require bigger electrode volumes than structural (relaxation) studies. Transmission resonances can be quite sensitive to the level spacing. To check for possible issues with level spacing, we have added new layers of Cu on the outer planes of both pyramids in successive steps and compared respective transmission functions. Figure 3 shows transmission for electrodes differing by the number of Cu atoms, N_{Cu}. We find that the salient features of the transmission curve turn out to be captured already with $N_{\mathrm{Cu}} = 18$. All transport data shown in the Results section have been obtained for this electrode size.

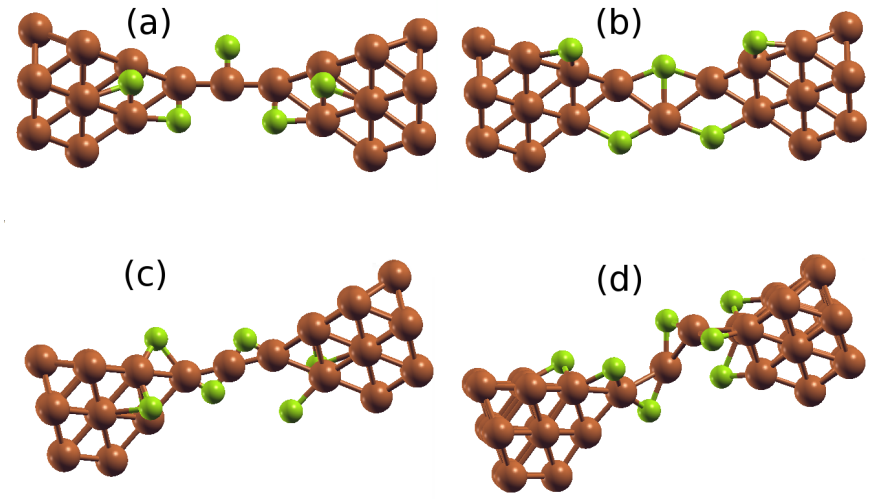

Figure 2: (a) Initial geometry, first structure. (b) Structure after relaxation of the central part of the junction, "unconstrained geometry", see text. (c) Initial geometry, second structure and (d) a corresponding relaxed structure.

Local density of states and electron transport

LDoS: copper junction The valence electronic structure of a copper atom is $[\mathrm{Ar}]4\mathrm{s}^1 3\mathrm{d}^{10}$. In Fig. 4, top-left, we plot the local (central atom) density of states for a clean Cu junction. As it is quite common with transition metals, the (quasi) d-band is clearly recognized in the LDoS as a pronounced ridge; for the Cu junction the ridge develops in the range $[-7., -1.]$ eV. We note that all the eigenstates in the energy window of several eV around E_{F} should be considered as spd hybrids. The eigenstates of the three Cu atoms – apices and central atom – can be classified according to the $\mathrm{C}_{\infty v}$ group of the two-dimensional

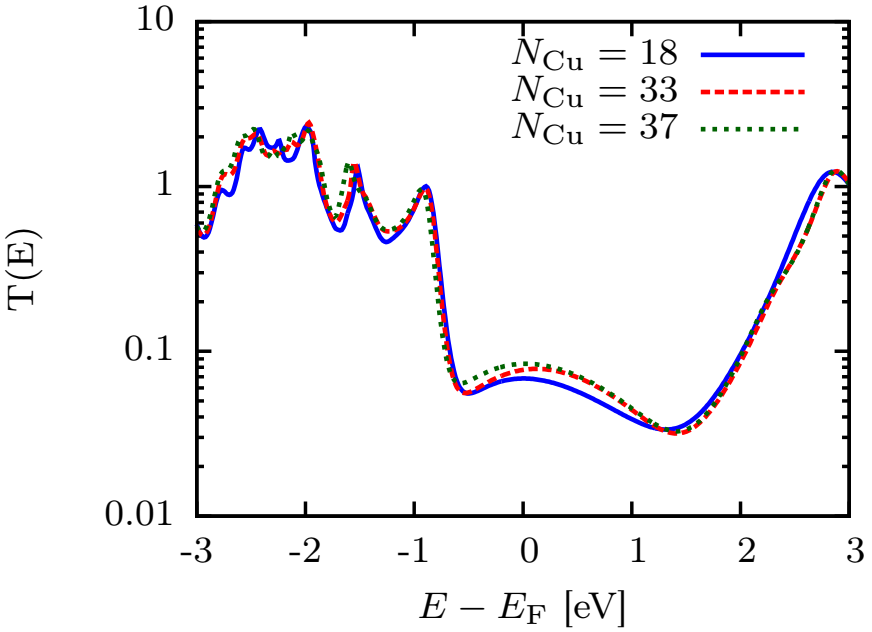

Figure 3: Convergence of the transmission function with respect to the cluster size. The number N_{Cu} refers to the amount of Cu atoms of the clusters. The structure contained Cl adsorbates with optimized positions (constrained relaxation).

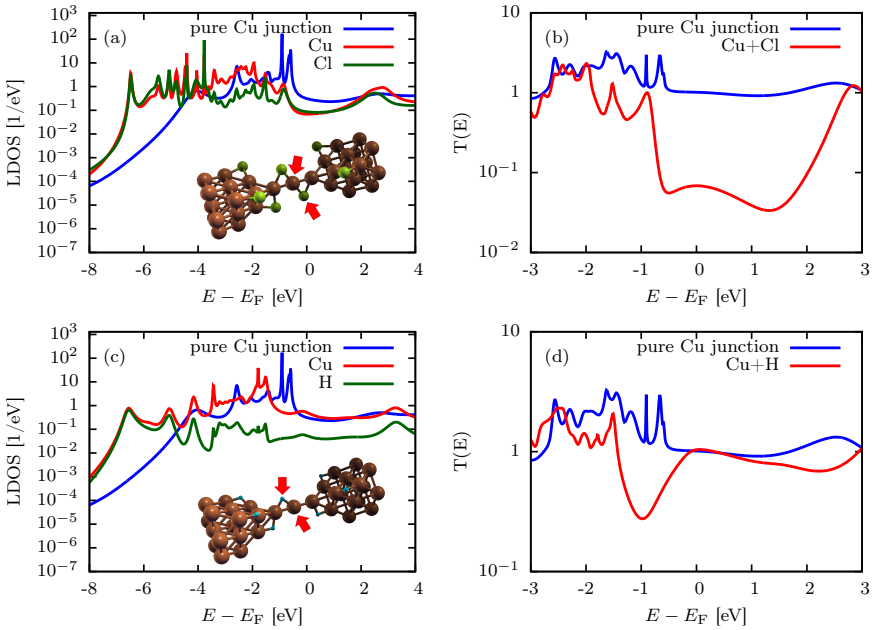

Figure 4: Local density of states (a,c) taken on the central part of the junction (red arrows in inset) and transmission (b,d) for constrained geometries with Cl-adsorbates (a,b) and H-adsorbates, (c,d). Blue traces correspond to reference data obtained for the junction without adsorbates. Additionally, LDoS on the adsorbates is shown by green traces.

rotor. The first three irreducible representations are Σ (atomic angular-momentum states $\mathrm{s}, \mathrm{p}_z, \mathrm{d}_{z^2}$), Π ($\mathrm{p}_x, \mathrm{p}_y, \mathrm{d}_{xz}, \mathrm{d}_{yz}$) and Δ ($\mathrm{d}_{xy}, \mathrm{d}_{x^2-y^2}$) with ascending angular momentum w.r.t. the z axis that goes through the three atoms. The inter-atomic hoppings decrease as the angular momentum increases. It is thus not surprising that the ridge consists of sharp spikes, as well as a relatively broad background. At $E = E_\mathrm{F}$ the Σ character is prominent, where it gives rise to a flat LDoS.

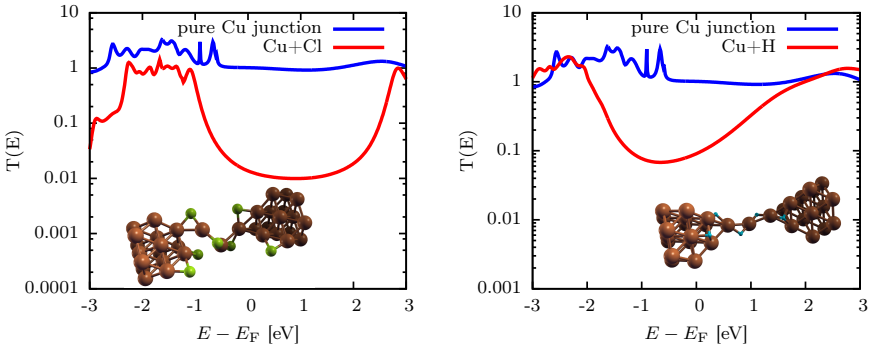

Figure 5: Comparison of transmission functions for a junction with adsorbates (red curves) and without adsorbates (blue curves). The central junction atoms were relaxed without constraints. Adsorption of Cl is addressed in the left panel, H in the right panel.

LDoS: wire with adsorbates After placing the adsorbates, the LDoS changes significantly, because the coordination number of the central Cu atom changes from two to four. In general, the copper orbitals may lower their energy as the bonds to adsorbates are formed. In turn, the LDoS at the Fermi level is depleted. If the geometry of the Cu backbone is held fixed, i.e., does not react to the adsorbates, then the effect turns out to be much stronger for the Cl atom as compared to H. Presumably, this is because Cl binds with 3p orbitals that rehybridize and thereby can optimize the overlap with the orbitals of Cu more efficiently than the single 1s-orbital of a proton. Interestingly, this qualitative difference between Cl and H adsorbates is largely erased once one allows the geometry of the Cu backbone to respond to the presence of adsorbates, see Fig. 5. When the Cu backbone reconstructs, then it does so by shifting Cu atoms in a way so as to optimize overlaps with all neighboring atoms. In this process, re-hybridization of the Cu orbitals can take better advantage of the protons, too,

and so the spectral gap near the Fermi energy is enhanced also with H adsorbates.

Transmission The clean wire has unity transmission at the Fermi level (Fig. 4, blue curve) indicating the presence of a single almost perfectly transmitting transport channel. This channel arises due to the Σ states discussed previously. The impact of adsorbates on the transmission is very strongly dependent on the adsorbate, if the geometry of the Cu backbone is held fixed, i.e., does not reconstruct. As we show in Fig. 4, in this situation the Cl atoms suppress the transmission by an order of magnitude, while the H adsorbates leave it almost invariant. Again, after relaxation of the Cu backbone this difference is erased and in both cases the transmission is strongly suppressed, see Fig. 5.

It is expected that the Cl-Cu bonds have a stronger polar character than H-Cu, implying stronger adsorption-induced electrostatic fields that act as potential barriers for electrons. This can be verified by a direct comparison of transmissions and LDoS in Fig. 4. On the H adsorption, the LDoS at E_{F} and $T(E_{\mathrm{F}})$ undergo very small changes. Due to the Cl adsorption, the LDoS at E_{F} is reduced by a factor ≈ 3, but $T(E_{\mathrm{F}})$ drops by a factor ≈ 12, indicating reflection of scattering electrons at the Cl barrier.

Conclusions and Outlook

We have investigated the transport through single-atom thick metal wires in an electrochemical environment. The model system that we have considered was a Cu wire in an environment with Cl and/or H ions. The amount of adatom coverage has been calculated for planar Cu(111) surface with DFT-based methods. The result served as an input for the construction of model geometries which have been underlying the electron transport calculation. We observe that adatoms have a drastic effect on the transmission of the atomic junction, because they tend to form a chemical bond with the central (bottleneck) metal atom. The bond formation, depletes the density of states locally within the junction, and as a consequence the transmission probability is decreased as well – in our example by more

than an order of magnitude.

It is expected that in nanowires with thickness of several atoms adsorption induced structural changes will be weak. In our opinion, in this case H adsorption will not change the conductance, while Cl will induce an observable decrease, as suggested by our analysis of the constrained structures. The obvious fact that the adsorbed ions influence especially the very thin single-atom junctions, may easily explain our experimental observation that in many cases it seems to be much easier to observe conductance in integer multiples of G_0 in larger junctions than in single-atom junctions.[1,35–38]

Our results have two relevant implications concerning the potential of electrochemical means to control the conductance of single-atom junctions made of under-coordinated noble metals (Cu, Ag, Au). (i) One suspects that the junction's reactivity is relatively high, so that electrochemical control with coverages exceeding significantly 10% and more might have to imply binding and unbinding of adsorbates right on the junction-forming metal atoms. (ii) Moreover, one may think about a mechanical control of the junction mediated by electrochemical means. For instance, a proposal based on electrochemical control of the surface tension has been made before.[1,35–38] Strain can significantly influence the adsorption properties of metal electrodes.[39,40] Controlling surface tension can result in conditions under which the contamination of the junction with solvent atoms might be sufficiently improbable so that the mechanism of transport suppression due to adatoms could be less relevant. This may explain the fact that according to our experimental findings, in the case of atomic transistors operated in this way, the influence of defect scattering in most cases is remarkably low.

For sure, the research field of quantum transport controlled by electrochemical means is still in its infancy. Many more studies, theoretical and experimental, on different combinations of materials and transport mechanisms will have to be performed, before its full potential could really reveal itself.

Acknowledgement

We acknowledge support by the Baden-Württemberg Stiftung within the Research Network "Functional Nanostructures". AB acknowledges support of DFG through the research grant AB 4265/2-1. PS, RK and FE gratefully acknowledge the Steinbuch Centre for Computing (SCC) for providing computing time on the computer HC3 at Karlsruhe Institute of Technology (KIT).

References

(1) Xie, F.-Q.; Nittler, L.; Obermair, C.; Schimmel, T. *Phys. Rev. Lett.* **2004**, *93*, 128303.

(2) Li, C.; Mishchenko, A.; Li, Z.; Pobelov, I.; Wandlowski, T.; Li, X. Q.; Würthner, F.; Bagrets, A.; Evers, F. *J. Phys. Condens. Matter* **2008**, *20*, 374122.

(3) Bagrets, A.; Arnold, A.; Evers, F. *J. Am. Chem. Soc.* **2008**, *130*, 9013–9018.

(4) Scullion, L.; Doneux, T.; Bouffier, L.; Fernig, D. G.; Higgins, S. J.; Bethell, D.; Nichols, R. J. *The Journal of Physical Chemistry C* **2011**, *115*, 8361–8368.

(5) Weissmüller, J.; Viswanath, R. N.; Kramer, D.; Zimmer, P.; Würschum, R.; Gleiter, H. *Science* **2003**, *300*, 312–315.

(6) Mancini, M.; Kubiak, P.; Wohlfahrt-Mehrens, M.; Marassi, R. *J. Electrochem. Soc.* **2010**, *157*, A164.

(7) Simeone, F. C.; Kolb, D. M.; Venkatachalam, S.; Jacob, T. *Angew. Chem. Int. Ed. Engl.* **2007**, *46*, 8903–8906.

(8) Chapman, D. L. *Philos. Mag.* **1913**, *25*, 475–481.

(9) Gouy, G. *J. Phys.* **1910**, *9*, 457–467.

(10) Kresse, G.; Furthmüller, J. *Phys. Rev. B. Condens. Matter* **1996**, *54*, 11169–11186.

(11) Perdew, J. P.; Burke, K.; Ernzerhof, M. *Phys. Rev. Lett.* **1996**, *77*, 3865.

(12) Blöchl, P. E. *Phys. Rev. B* **1994**, *50*, 17953.

(13) Kresse, G.; Joubert, D. *Phys. Rev. B* **1999**, *59*, 1758.

(14) Monkhorst, H. J.; Pack, J. D. *Phys. Rev. B* **1976**, *13*, 5188.

(15) Methfessel, M.; Paxton, A. T. *Phys. Rev. B* **1989**, *40*, 3616.

(16) Koper, M. T. M.; van Santen, R. A. *Surf. Sci.* **1999**, *422*, 118.

(17) Peljhan, S.; Koller, J.; Kokalj, A. *J. Phys. Chem. C* **2014**, *118*, 933–943.

(18) Nørskov, J. K.; Rossmeisl, J.; Logadottir, A.; Lindqvist, L.; Kitchin, J. R.; Bligaard, T.; Jónsson, H. *J. Phys. Chem. B* **2004**, *108*, 17886–17892.

(19) Nørskov, J. K.; Bligaard, T.; Logadottir, A.; Kitchin, J. R.; Chen, J. G.; Pandelov, S.; Stimming, U. *J. Electrochem. Soc.* **2005**, *152*, J23.

(20) Gossenberger, F.; Roman, T.; Groß, A. *Surf. Sci.* **2014**,

(21) Sakong, S.; Groß, A. *Surf. Sci.* **2003**, *525*, 107.

(22) Greeley, J.; Mavrikakis, M. *J. Phys. Chem. B* **2005**, *109*, 3460.

(23) Peljhan, S.; Kokalj, A. *J. Phys. Chem. C* **2009**, *113*, 14363–14376.

(24) Roman, T.; Gossenberger, F.; Forster-Tonigold, K.; Groß, A. *Phys. Chem. Chem. Phys.* **2014**, *16*, 13630.

(25) Kruft, M.; Wohlmann, B.; Stuhlmann, C.; Wandelt, K. *Surf. Sci.* **1997**, *377-379*, 601.

(26) Wohlmann, B.; Park, Z.; Kruft, M.; Stuhlmann, C.; Wandelt, K. *Colloids Surf. A* **1998**, *134*, 15.

(27) Groß, A. *Surf. Sci.* **2013**, *608*, 249 – 254.

(28) Quaino, P.; Juarez, F.; Santos, E.; Schmickler, W. *Beilstein J. Nanotechnol.* **2014**, *5*, 846–854.

(29) Roman, T.; Groß, A. *Catalysis Today* **2013**, *202*, 183–190.

(30) Blum, V.; Gehrke, R.; Hanke, F.; Havu, P.; Havu, V.; Ren, X.; Reuter, K.; Scheffler, M. *Comput. Phys. Commun.* **2009**, *180*, 2175–2196.

(31) Arnold, A.; Weigend, F.; Evers, F. *J. Chem. Phys.* **2007**, *126*, 174101.

(32) Bagrets, A. *J. Chem. Theory Comput.* **2013**, *9*, 2801–2815.

(33) Wilhelm, J.; Walz, M.; Stendel, M.; Bagrets, A.; Evers, F. *Phys. Chem. Chem. Phys.* **2013**, *15*, 6684–6690.

(34) Evers, F.; Schmitteckert, P. *EPL (Europhysics Lett.)* **2013**, *103*, 47012.

(35) H. Gleiter, H. H., Th. Schimmel *Nano Today* **2014**, *9*, 17–68.

(36) Maul, R.; Xie, F.-Q.; Obermair, C.; Schön, G.; Schimmel, T.; Wenzel, W. *Applied Physics Letters* **2012**, *100*, –.

(37) Xie, F.-Q.; Hüser, F.; Pauly, F.; Obermair, C.; Schön, G.; Schimmel, T. *Phys. Rev. B* **2010**, *82*, 075417.

(38) Xie, F.; Maul, R.; Obermair, C.; Wenzel, W.; Schn, G.; Schimmel, T. *Advanced Materials* **2010**, *22*, 2033–2036.

(39) Mavrikakis, M.; Hammer, B.; Nørskov, J. K. *Phys. Rev. Lett.* **1998**, *81*, 2819.

(40) Groß, A. *Topics in Catalysis* **2006**, *37*, 29–39.

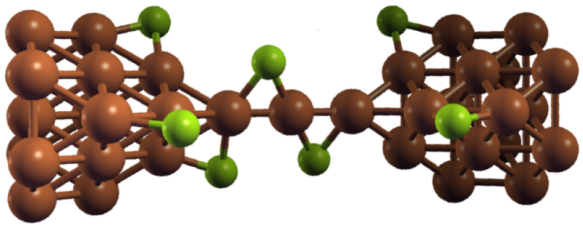

Table of Contents Image